

**ZINC SELENITES: THE SOLUBILITY DIAGRAM AND ITS USE  
FOR THE ISOLATION OF THE COMPOUNDS,  
THEIR SPECTRAL FEATURES AND THERMAL BEHAVIOUR  
AND THE STRENGTH OF BONDS IN THEM**

Miroslav EBERT, Zdeněk MIČKA and Marcela UCHYTILOVÁ

*Department of Inorganic Chemistry,  
Charles University, 128 40 Prague 2*

Received March 2nd, 1983

The solubility diagrams of the  $\text{ZnSeO}_3\text{--SeO}_2\text{--H}_2\text{O}$  system were obtained at 0 and 25°C and utilized for the preparation of  $\text{Zn}(\text{HSeO}_3)_2\cdot 2\text{H}_2\text{O}$  and  $\text{ZnSe}_2\text{O}_5$ , respectively. The thermal stability and the infrared absorption spectra were studied for  $\text{ZnSeO}_3$ ,  $\text{Zn}(\text{HSeO}_3)_2\cdot 2\text{H}_2\text{O}$ , and  $\text{ZnSe}_2\text{O}_5$ , and the force constants of the selenium-oxygen bonds were evaluated and the hydrogen bonds present were characterized.

As part of a systematic study of selenites as potential ferroelectrics, the present work is devoted to zinc selenites. The ferroelectric behaviour of hydrogenselenites is closely related with the nature of the hydrogen bonds involved. Therefore, studying the  $\text{ZnSeO}_3\text{--SeO}_2\text{--H}_2\text{O}$  system we focussed our interest particularly on the hydrogen-selenites present, with emphasis on the hydrogen bonding occurring in them. The transformation of zinc hydrogenselenite to diselenite in dependence on temperature was also of interest.

Some of the zinc selenites dealt with in this work have been prepared<sup>1-7</sup> and their structure and/or infrared spectra discussed<sup>8-11</sup>. We directed our attention to the solubility diagrams of the  $\text{ZnSeO}_3\text{--SeO}_2\text{--H}_2\text{O}$  system and to the synthesis of selenites whose existence is revealed by this diagram.

**EXPERIMENTAL**

Anhydrous zinc selenite and selenium dioxide (both reagent grade chemicals of Lachema, Brno) were used.  $\text{Zn}(\text{HSeO}_3)_2\cdot 2\text{H}_2\text{O}$  and  $\text{ZnSe}_2\text{O}_5$  were isolated based on the solubility diagrams of the  $\text{ZnSeO}_3\text{--SeO}_2\text{--H}_2\text{O}$  system at 0°C and 25°C, respectively.  $\text{ZnSe}_2\text{O}_5$  was freed from selenious acid by agitating it with chloroform for several hours. The two compounds isolated were collected on an S4 sintered glass filter, washed with chloroform, and dried:  $\text{Zn}(\text{HSeO}_3)_2\cdot 2\text{H}_2\text{O}$  in a desiccator over  $\text{H}_2\text{SO}_4$  at 0°C,  $\text{ZnSe}_2\text{O}_5$  in air at room temperature. The substances form white, fine crystals, well soluble in dilute acids and transforming into  $\text{ZnSeO}_3$  when in contact with water. For  $\text{Zn}(\text{HSeO}_3)_2\cdot 2\text{H}_2\text{O}$  calculated: 18.29% Zn, 44.19% Se; found: 17.93% Zn, 43.83% Se, for  $\text{ZnSe}_2\text{O}_5$  calculated: 21.55% Zn, 52.07% Se; found: 22.24% Zn, 51.19% Se.  $\text{Zn}(\text{DSeO}_3)_2\cdot 2\text{D}_2\text{O}$  was prepared from  $\text{ZnSeO}_3$ ,  $\text{SeO}_2$ , and  $\text{D}_2\text{O}$ .

The starting chemicals were analyzed gravimetrically; selenium was determined by an adapted method after Bode<sup>12</sup>, zinc, as  $Zn_2P_2O_7$  after its precipitation with ammonium phosphate and annealing<sup>13</sup>. The titrimetric approach was applied to the solubility study: selenium(IV) was determined iodometrically<sup>14</sup>, zinc, chelatometrically in Schwarzenbach's buffer solution using Eriochrome Black T as indicator<sup>15</sup>.

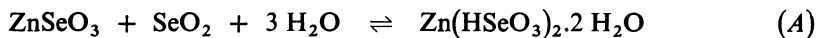
The infrared spectra were recorded on a UR 20 spectrophotometer (Carl Zeiss, Jena) over the region of  $400-4000\text{ cm}^{-1}$ . Nujol mulls were measured in potassium bromide cells; tripene mulls were also used in the  $1600-4000\text{ cm}^{-1}$  range.

The thermal behaviour of the substances was examined thermogravimetrically and by differential thermal analysis, using a Derivatograph instrument (MOM, Budapest); temperature region  $25-600^\circ\text{C}$ , linear temperature sweep of  $5^\circ\text{C}/\text{min}$ .

## RESULTS AND DISCUSSION

The solubility in the  $ZnSeO_3$ - $SeO_2$ - $H_2O$  system was studied at  $0^\circ\text{C}$  and  $25^\circ\text{C}$  by the Schreinemakers method; the equilibrium established in 1–2 months. The diagrams were plotted according to Gibbs and Roozenboom.

The solubility diagram at  $0^\circ\text{C}$  is shown in Fig. 1. In addition to the starting substances,  $ZnSeO_3$  and  $SeO_2$  (crystallization fields I and V, respectively), an incongruently soluble selenite is also formed (crystallization field III). The equilibria between two solids and the solutions of the composition of the peritonic point  $P$  (3.8%  $ZnSeO_3$ , 6.2%  $SeO_2$ , 90.0%  $H_2O$ ) or the eutonic point  $E$  (6.5%  $ZnSeO_3$ , 54.9%  $SeO_2$ , 38.6%  $H_2O$ ) are described by fields II and IV, respectively. The incongruently soluble selenite is formed in the highest yield if the starting substances are present in the molar ratio  $ZnSeO_3 : H_2SeO_3 : H_2O = 1.0 : 2.1 : 17.1$ , and its composition is given by the ratio  $Zn : Se : H_2O = 1 : 2 : 3$ . A compound of this composition has been obtained first by Boutzoureano<sup>6</sup>. Lieder and Gattow<sup>16</sup> report its structure as  $ZnSe_2O_5 \cdot 3 H_2O$ , Kondrashev and Nozik<sup>8</sup>, as  $Zn(HSeO_3)_2 \cdot 2 H_2O$ . The latter structure is confirmed by our infrared spectra (Table I). Thus, the reaction



takes place at  $0^\circ\text{C}$  in field II with the liquid phase composition corresponding to the peritonic point.

The solubility diagram for  $25^\circ\text{C}$  is shown in Fig. 2. Again, in addition to the initial compounds (crystallization fields I and V), an incongruently soluble compound is formed, associated with crystallization field III, and fields II and IV pertain to the equilibria between two solids and the solutions of the composition of the peritonic point  $P$  (4.3%  $ZnSeO_3$ , 42.0%  $SeO_2$ , 53.7%  $H_2O$ ) or the eutonic point  $E$  (2.9%  $ZnSeO_3$ , 65.5%  $SeO_2$ , 31.6%  $H_2O$ ). The molar ratio leading to the highest yield of the new compound is  $ZnSeO_3 : H_2SeO_3 : H_2O = 1.0 : 2.6 : 6.4$ , the ratio of the constituents is  $Zn : Se = 1 : 2$ . The infrared spectra (Table II) give evidence that the compound is  $ZnSe_2O_5$ . Hence, in field II, with the liquid phase composition

TABLE I

Infrared band positions ( $\text{cm}^{-1}$ ) and relative intensities for  $\text{Zn}(\text{HSeO}_3)_2 \cdot 2 \text{H}_2\text{O}$  and  $\text{Zn}(\text{DSeO}_3)_2 \cdot 2 \text{D}_2\text{O}$ . Symbols: vs very strong, s strong, m medium, w weak, v w very weak, b broad, sh shoulder;  $\nu_s$ ,  $\nu_{as}$  symmetric and antisymmetric stretching,  $\delta$  bending,  $\varrho$  rocking vibration

$\tilde{\nu}(\text{Zn}(\text{HSeO}_3)_2 \cdot 2 \text{H}_2\text{O})$	$\tilde{\nu}(\text{Zn}(\text{DSeO}_3)_2 \cdot 2 \text{D}_2\text{O})$	$\frac{\tilde{\nu}(\text{H})^a}{\tilde{\nu}(\text{D})}$	Assignment <sup>b</sup>
400 m	400 s	1.00	
442 s	415 sh	1.06	$\delta(\text{SeO}_2)$
470 s	463 s	1.01	
—	530 s	—	$\varrho(\text{X}_2\text{O})$
668 vs	657 vs	1.01	$\nu(\text{SeO})(\text{SeOX})$
745 vs	735 vs	1.01	$\nu_{as}(\text{SeO}_2)$
817 s	804 s	1.02	
	810 sh		$\nu_s(\text{SeO}_2)$
1 196 m	885 s	1.35	$\delta(\text{OX})(\text{SeOX})$
1 638 m	1 203 m	1.36	$\delta(\text{OX})(\text{X}_2\text{O})$
2 380 wb	1 760 wb	1.35	
2 600—3 200 vb <sup>c</sup>	1 900—2 300 vb <sup>d</sup>	1.39	$\nu(\text{OX})(\text{SeOX})$
3 350—3 650 vb <sup>e</sup>	2 500—2 700 vb <sup>f</sup>	1.34	$\nu(\text{OX})(\text{X}_2\text{O})$

<sup>a</sup>  $\tilde{\nu}(\text{Zn}(\text{HSeO}_3)_2 \cdot 2 \text{H}_2\text{O})/\tilde{\nu}(\text{Zn}(\text{DSeO}_3)_2 \cdot 2 \text{D}_2\text{O})$ ; <sup>b</sup> X = H, D; <sup>c</sup> max. 3 050  $\text{cm}^{-1}$ ; <sup>d</sup> max. 2 200  $\text{cm}^{-1}$ ; <sup>e</sup> max. 3 430  $\text{cm}^{-1}$ ; <sup>f</sup> max. 2 550  $\text{cm}^{-1}$ .

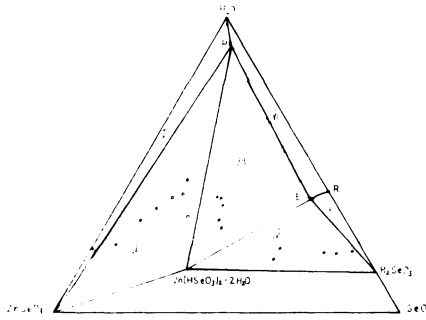


FIG. 1

Solubility diagram for the  $\text{ZnSeO}_3\text{--SeO}_2\text{--H}_2\text{O}$  system at  $0^\circ\text{C}$

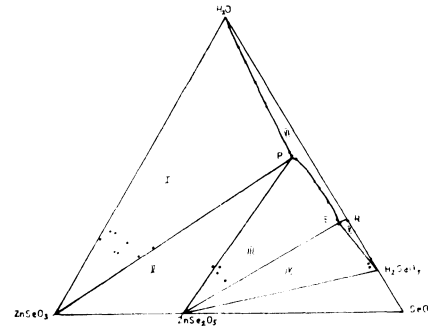
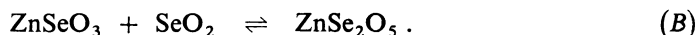


FIG. 2

Solubility diagram for the  $\text{ZnSeO}_3\text{--SeO}_2\text{--H}_2\text{O}$  system at  $25^\circ\text{C}$

as given by point *P*, a reaction proceeds resulting in the formation of diselenite,



Thus, lower temperatures favour the formation of hydrogenselenite, whereas diselenite is formed preferentially at higher temperatures. Under similar conditions, the formation of diselenite at 25°C has only been observed with barium<sup>17</sup>, whereas with alkali metals<sup>18</sup>, magnesium<sup>19</sup>, calcium<sup>20</sup>, strontium<sup>17</sup>, cobalt<sup>21</sup>, and nickel<sup>22</sup> selenites, only hydrogenselenites have been obtained at this temperature.

The thermal analysis curves of  $\text{ZnSeO}_3$  display a minor mass loss over the region of 170–210°C (Table III), due to a partial decomposition of the substance; a similar effect has been observed with alkali selenites<sup>18</sup>. A complete decomposition of zinc selenite occurs at 490°C. The decomposition of zinc hydrogenselenite dihydrate over the range of 10–90°C leads to zinc diselenite, which, releasing selenium dioxide, decomposes at 290–360°C to zinc selenite. The zinc diselenite obtained based on the solubility study decomposes likewise.

Based on the spectral band positions for the stretching vibrations of the  $\text{SeO}_3$ ,  $\text{SeO}_2$ ,  $\text{SeOH}$ , and  $\text{Se}-\text{O}-\text{Se}$  groups, the force constants of the  $\text{Se}-\text{O}$  bonds were calculated making use of Lehmann's relation<sup>23</sup>, applied previously to magnesium selenites<sup>19</sup>. The bond strength (Table IV) is seen to decrease in order  $\text{SeO}_2(\text{Se}_2\text{O}_5^{2-}) > > \text{SeO}_2(\text{HSeO}_3^-) > \text{SeO}_3 > \text{SeOH} > \text{Se}-\text{O}-\text{Se}$ . This is consistent with the results obtained for other selenites<sup>17–22</sup>. Comparing the values of the force constant in the  $\text{SeOH}$  group in the series of divalent metal hydrogenselenites we find the  $\text{Se}-\text{O}$  bond

TABLE II  
Infrared band positions ( $\text{cm}^{-1}$ ) and relative intensities for  $\text{ZnSeO}_3$  and  $\text{ZnSe}_2\text{O}_5$ . Symbol as in Table I

$\tilde{\nu}(\text{ZnSeO}_3)$	Assignment	$\tilde{\nu}(\text{ZnSe}_2\text{O}_5)$	Assignment
405 vw 487 m 535 m	$\delta(\text{SeO}_3)$	448 s 531 sh 553 vs	$\delta(\text{SeO})_2$ $\nu_s(\text{Se}-\text{O}-\text{Se})$
703 vs 730 vs 763 s	$\nu_{as}(\text{SeO}_3)$	597 s 747 vs 777 sh	$\nu_{as}(\text{Se}-\text{O}-\text{Se})$ $\nu_{as}(\text{SeO}_2)$
826 s 850 s	$\nu_s(\text{SeO}_3)$	830 s 849 m 887 s	$\nu_s(\text{SeO}_2)$

TABLE III  
Thermal decomposition of zinc selenites

Temperature °C	TGA	DTA	Assignment
<b>ZnSeO<sub>3</sub></b>			
25—170	plateau	—	ZnSeO <sub>3</sub>
170—210	loss 0·6%	endo	partial decomposition
210—485	plateau	—	—
485—600	loss 31·7%	endo	decomposition and liberation of SeO <sub>2</sub>
<b>Zn(HSeO<sub>3</sub>)<sub>2</sub>.2 H<sub>2</sub>O</b>			
10—90	loss 12·4%	endo	loss of H <sub>2</sub> O
90—200	plateau	—	ZnSe <sub>2</sub> O <sub>5</sub>
200—240	loss 14·5%	endo	partial decomposition
240—285	plateau	—	—
285—355	loss 44·3%	endo	decomposition and liberation of SeO <sub>2</sub>
355—480	plateau	—	ZnSeO <sub>3</sub>
480—600	loss 76·6%	endo	decomposition and liberation of SeO <sub>2</sub>
<b>ZnSe<sub>2</sub>O<sub>5</sub></b>			
25—280	plateau	—	ZnSe <sub>2</sub> O <sub>5</sub>
280—385	loss 36·5%	endo	decomposition and liberation of SeO <sub>2</sub>
385—490	plateau	—	ZnSeO <sub>3</sub>
490—590	loss 57·9%	endo	decomposition and liberation of SeO <sub>2</sub>

TABLE IV  
Force constants (N m<sup>-1</sup>) of the selenium–oxygen bonds in zinc selenites

Compound	Group	<i>K<sub>Se–O</sub></i>
ZnSeO <sub>3</sub>	SeO <sub>3</sub>	464
Zn(HSeO <sub>3</sub> ) <sub>2</sub> .2 H <sub>2</sub> O	SeO <sub>2</sub>	480
	SeOH	350
ZnSe <sub>2</sub> O <sub>5</sub>	SeO <sub>2</sub>	526
	Se–O–Se	241

strongest just in zinc hydrogenselenite dihydrate. Consequently, the O—H group is here weakest and so it is broken down most readily to give the diselenite Se—O—Se group and release water. This is why diselenite is found in the heterogeneous  $\text{ZnSeO}_3$ — $\text{SeO}_2$ — $\text{H}_2\text{O}$  system at 25°C, hydrogenselenite appearing only at lower temperatures. The bonding properties also reflect in the substantially lower temperature of decomposition of  $\text{Zn}(\text{HSeO}_3)_2 \cdot 2 \text{H}_2\text{O}$  giving  $\text{ZnSe}_2\text{O}_5$  and releasing water, as compared with the analogous  $\text{Co}(\text{HSeO}_3)_2 \cdot 2 \text{H}_2\text{O}$  and  $\text{Ni}(\text{HSeO}_3)_2 \cdot 2 \text{H}_2\text{O}$ . While the zinc salt decomposes at 10–90°C, the cobalt and nickel salts, possessing considerably lower  $K_{\text{Se}-\text{O}}$  values in the SeOH groups, decompose at temperatures as high as 80–200°C.

As follows from the structural analysis<sup>8</sup>, two water-anion hydrogen bonds  $279.3 \pm \pm 0.5$  and  $266.1 \pm 0.4$  pm long and an anion-anion bond  $265.7 \pm 0.5$  pm long are present in  $\text{Zn}(\text{HSeO}_3)_2 \cdot 2 \text{H}_2\text{O}$ . Consistent with this are our data obtained *via* the  $\nu_{\text{OH}}$  vs  $R_{\text{O...O}}$  correlation diagrams based on the wavenumbers of the OH stretching vibrations<sup>24–28</sup>. The bond lengths thus obtained are 285–280 pm and 271–266 pm. These values class the hydrogen bonds in question among weak to medium ones, and are in accordance with the data obtained for other divalent metal hydrogenselenites<sup>17,19–22</sup>.

#### REFERENCES

1. Berzelius J. J.: *Ann. Chim. Phys.* 9, 160, 225, 266, 337 (1818).
2. Berzelius J. J.: *Ann. Mines* 4, 301 (1819).
3. Muspratt J. S.: *Justus Liebigs Ann. Chem.* 70, 275 (1849).
4. Nilson L. F.: *Bull. Soc. Chim. Fr.* 21, 253 (1874).
5. Nilson L. F.: *Bull. Soc. Chim. Fr.* 23, 262, 357 (1875).
6. Boutzoureano B.: *Ann. Chim. Phys.* 18, 289 (1889).
7. Wöhler F.: *Justus Liebigs Ann. Chem.* 63, 279 (1847).
8. Kondrashev J. D., Nozik J. Z.: *Kristallografiya* 24, 586 (1979).
9. Meunier G., Bertrand M.: *Acta Crystallogr. B* 30, 2840 (1974).
10. Sathianandan K., McCory L. D., Margrave J. L.: *Spectrochim. Acta A* 20, 957 (1964).
11. Muldagalieva R. A., Shokanov A. K.: *Tr. Khim. Met. Inst. Akad. Nauk Kaz. SSSR* 22, 16 (1973).
12. Bode H.: *Z. Anal. Chem.* 153, 335 (1956).
13. Tomíček O.: *Kvantitativní analýza*. Published by SZN, Prague 1954.
14. Ganitskii M. Zh., Zelinokrayte V. I.: *Zh. Neorg. Khim.* 2, 1341 (1957).
15. Přibil R.: *Komplexony v chemické analyse*. Published by Nakladatelství ČSAV, Prague 1957.
16. Lieder V. J., Gattow G.: *Naturwissenschaften* 54, 318 (1967).
17. Ebert M., Havlíček D.: *This Journal* 47, 1923 (1982).
18. Mička Z.: *Thesis*. Charles University, Prague 1982.
19. Ebert M., Havlíček D.: *Chem. Zvesti* 34, 441 (1980).
20. Ebert M., Havlíček D.: *This Journal* 46, 1740 (1981).
21. Ebert M., Mička Z., Peková I.: *Chem. Zvesti* 36, 160 (1982).
22. Ebert M., Mička Z., Peková I.: *This Journal* 47, 2069 (1982).
23. Lehmann W. J.: *J. Mol. Spectrosc.* 7, 261 (1961).

24. Naberukhin Yu. I., Efimov Yu. Ya.: *Zh. Strukt. Khim.* **12**, 591 (1971).
25. Pirrene J.: *Physica (Utrecht)* **21**, 971 (1955).
26. Novak A.: *Struct. Bond.* **18**, 177 (1974).
27. Ratajczak H., Orville-Thomas W. J.: *J. Mol. Struct.* **1**, 449 (1967/68).
28. Nakamoto K., Margoshes M., Rundle R. E.: *J. Amer. Chem. Soc.* **77**, 6480 (1955).

Translated by P. Adámek.